Ann. Occup. Hyg., Vol. 54, No. 5, pp. 514–531, 2010

doi:10.1093/annhyg/meq015

Aerosol Monitoring during Carbon Nanofiber Production: Mobile Direct-Reading Sampling

DOUGLAS E. EVANS*, BON KI KU, M. EILEEN BIRCH and KEVIN H. DUNN

Division of Applied Research and Technology, National Institute for Occupational Safety and Health, 4676 Columbia Parkway, MS-R5, Cincinnati, OH 45226, USA

Received 19 August 2009; in final form 16 February 2010; published online 6 May 2010

Detailed investigations were conducted at a facility that manufactures and processes carbon nanofibers (CNFs). Presented research summarizes the direct-reading monitoring aspects of the study. A mobile aerosol sampling platform, equipped with an aerosol instrument array, was used to characterize emissions at different locations within the facility. Particle number, respirable mass, active surface area, and photoelectric response were monitored with a condensation particle counter (CPC), a photometer, a diffusion charger, and a photoelectric aerosol sensor, respectively. CO and CO_2 were additionally monitored. Combined simultaneous monitoring of these metrics can be utilized to determine source and relative contribution of airborne particles (CNFs and others) within a workplace. Elevated particle number concentrations, up to 1.15×10^6 cm^{-3}, were found within the facility but were not due to CNFs. Ultrafine particle emissions, released during thermal treatment of CNFs, were primarily responsible. In contrast, transient increases in respirable particle mass concentration, with a maximum of 1.1 mg m^{-3}, were due to CNF release through uncontrolled transfer and bagging. Of the applied metrics, our findings suggest that particle mass was probably the most useful and practical metric for monitoring CNF emissions in this facility. Through chemical means, CNFs may be selectively distinguished from other workplace contaminants (Birch *et al.*, in preparation), and for direct-reading monitoring applications, the photometer was found to provide a reasonable estimate of respirable CNF mass concentration. Particle size distribution measurements were conducted with an electrical low-pressure impactor and a fast particle size spectrometer. Results suggest that the dominant CNF mode by particle number lies between 200 and 250 nm for both aerodynamic and mobility equivalent diameters. Significant emissions of CO were also evident in this facility. Exposure control recommendations were described for processes as required.

Keywords: carbon monoxide; emissions; exposure; exposure controls; nanofibers; nanomaterial; nanoparticle; nanotubes; occupational; ultrafine; workplace

INTRODUCTION

The nanotechnologies are estimated to account for up to $4.0 trillion worth of manufactured goods by 2015, representing a compound annual growth rate of 41% (Lux Research, 2008). Some estimates project that unprecedented growth in this sector will require up to 2 million workers globally, with at least 800 000 of these in the USA alone (Roco and Bainbridge, 2005). The nanotechnologies find diverse use in high-performance intermediates, such as coatings and composites for aerospace, automobiles, and construction, and in electronics, displays, batteries, and healthcare. Second only to ceramics and metal oxides, carbon nanotubes (CNTs) will likely constitute a $460 million market by 2011 (Holman *et al.*, 2007).

CNFs cost significantly less than CNTs to produce, are advantageous when compared to CNTs in

*Author to whom correspondence should be addressed.
Tel: +1-513-841-4407; fax: +1-513-841-4545;
e-mail: dje3@cdc.gov

certain applications, and can provide a high performance to cost ratio. With conventional milled carbon fibers (5–10 μm diameter) and single-walled carbon nanotubes (SWCNTs) (1–10 nm diameter), CNFs lie between these two materials in size, with typical diameters on the order of 50–200 nm (Ku *et al.*, 2006). CNFs may possess lengths from tens of micrometer to several centimeters, average aspect ratios of >100, and display various morphologies, including cupped or stacked graphene structures.

CNFs and multiwalled carbon nanotubes (MWCNTs), however, are structurally similar in several ways. MWCNTs possess diameters up to 100 nm (Wang *et al.*, 2006); both possess hollow cores and display either discrete or bundled fibrous morphologies (Ku *et al.*, 2006; Wang *et al.*, 2007). In contrast, SWCNTs, with less rigid structure, have a strong tendency to form nonfibrous bundles and ropes (Shvedova *et al.*, 2005; Maynard *et al.*, 2007). The primary characteristic that distinguishes CNFs from CNTs resides in graphene plane alignment. If the graphene plane and fiber axis do not align, the structure is defined as a CNF, but when parallel, the structure is considered a CNT (ISO/TS 27687:2008, 2008).

Industrial high-volume production presents the potential for worker exposure, especially those involved in the manual handling, transfer, or conveyance of these materials. Inhalation of aerosolized material is expected to be the primary route of exposure and is of most concern. Despite rapid growth in the nanotechnologies, relatively little is known about potential adverse health effects or exposures. A number of recent toxicological studies have focused on SWCNTs or MWCNTs. Inflammation, rapid pulmonary fibrosis, granulomas, oxidative stress, and mutagenesis have all been observed in the lungs of mice challenged with SWCNTs (Shvedova *et al.*, 2005, 2008). In addition, dermal inflammation (Murray *et al.*, 2009) has been documented. Concerns have also been raised regarding the asbestos-like pathogenicity of MWCNTs (Poland *et al.*, 2008).

Recent observations suggest that CNFs may induce acute inflammation and early onset of pulmonary fibrosis in mice exposed via pharyngeal aspiration (Kisin *et al.*, 2010). Because large-scale commercial production of CNFs is already under way, and little research has been conducted to date on emissions or exposure to CNFs in workplaces, there is an urgent need for this information.

The primary objective of this study was the identification, characterization, and differentiation of contaminant sources (CNF and others) within a CNF manufacturing facility. Personal exposure measurements and chemical and microscopic analyses of contaminants (through time-integrated sampling) are reported elsewhere (Birch *et al.*, in preparation). A secondary objective of the study was the assessment of direct-reading instrumentation and of the applied metrics (mass, surface area, number, and photoelectric response) for monitoring CNFs and other contaminants. A primary focus in this article was on the portable instruments employed since these may be more widely available for routine use. Specifically explored in this article was whether the instruments and differences in the particle properties/metrics utilized may potentially be used to differentiate emission plumes, their sources, and relative contributions in a workplace.

APPROACH

A better understanding of emissions and exposure to contaminants in workplaces may be gained through a combination of time-integrated and direct-reading sampling. Direct-reading monitors are essential for developing an understanding of 'how' contaminant emissions or exposures occur in addition to determining location. An observed elevation in a contaminant's concentration related to a particular event, process or task, aids in the identification of the underlying cause. Not only is identification critical for risk assessment but also for implementing effective and targeted control strategies to eliminate or reduce worker exposure.

In the context of workplaces where nanomaterials are manufactured, processed, or handled, there is not yet a clear consensus on which particle exposure metric or metrics should be monitored. It has been proposed that at a minimum, particle metrics of number, surface area, and mass be simultaneously monitored when attempting to assess nanomaterial exposure (Maynard and Kuempel, 2005; Oberdörster *et al.*, 2005). As a practical matter, workplace surveys are typically limited to 'area' or 'static' sampling when monitoring multiple metrics (Brouwer *et al.*, 2004). In manufacturing workplaces, processes often produce a signature aerosol, that is, an aerosol with a specific size profile (Dasch *et al.*, 2005) and/or a chemical fingerprint (Vincent, 2007). Contaminant transport and potential for inhaled dose may be more fully understood if an aerosol size characterization is performed.

Following an initial walk-through survey of a CNF manufacturing facility, several detailed surveys were subsequently conducted. A variety of direct-reading instruments and time-integrated samples (filters, sorbents, and microscopy collection media) were

employed to monitor personal exposures and process emissions. Direct-reading monitoring results from the sampling platform are reported here, while time-integrated chemical and microscopy results are described elsewhere (Birch *et al.*, in preparation). Particle number concentration, respirable mass, photoelectric response, and active surface area were monitored using a CPC, a photometer, a photoelectric aerosol sensor, and a diffusion charger, respectively. As general air quality indicators, CO, CO_2, temperature, and relative humidity were also monitored. In addition, real-time particle size distributions by number were measured using an electrical low-pressure impactor (ELPI) and a fast particulate size spectrometer (FPSS).

FACILITY DESCRIPTION

Manufacturing and processing operations were housed within a 5.5-m high, 2000-m^2 open structure. A facility floor plan is illustrated in Fig. 1. Annual CNF production totaled some 14 000 kg $year^{-1}$. No walls or other physical barriers between the different manufacturing areas were present. An administration section consisting of two floors was partitioned from the rest of the facility. Sampling took place throughout the facility on the ground floor. A process flow diagram illustrating the sequence of operations is provided in Fig. 2. A more detailed description of processes is provided in the Appendix 1.

Heating, cooling, ventilation, and other particle sources

Waste process heat generally maintained the manufacturing area at acceptable temperatures during winter. A manually controlled gas-fired radiant heater was mounted above the processing area to provide supplemental heating and operated for a short duration on one occasion during measurements. Direct-fired gas heating system efficiencies may exceed 90% [American Conference of Governmental Industrial Hygienists (ACGIH), 2007]. However, they may also act as significant ultrafine particle sources (Peters *et al.*, 2006, Heitbrink *et al.*, 2007; Evans *et al.*, 2008).

General ventilation in the production area was provided by three 1.5-kW roof-level exhaust fans but typically not in operation during colder months (when measurements described here were taken). No dedicated makeup air system was present to replace air removed by the roof exhaust fans or local exhaust systems. During warmer months, with roof fans in operation, unconditioned makeup air entered the building through open windows located to the west side of the facility. During cooler months, unconditioned makeup air from outdoors entered the facility through openings and gaps in the building structure. Air movement was not generally perceivable when standing in the manufacturing area since major local exhaust duct inlets were closer to roof rather than ground level. A battery-powered forklift

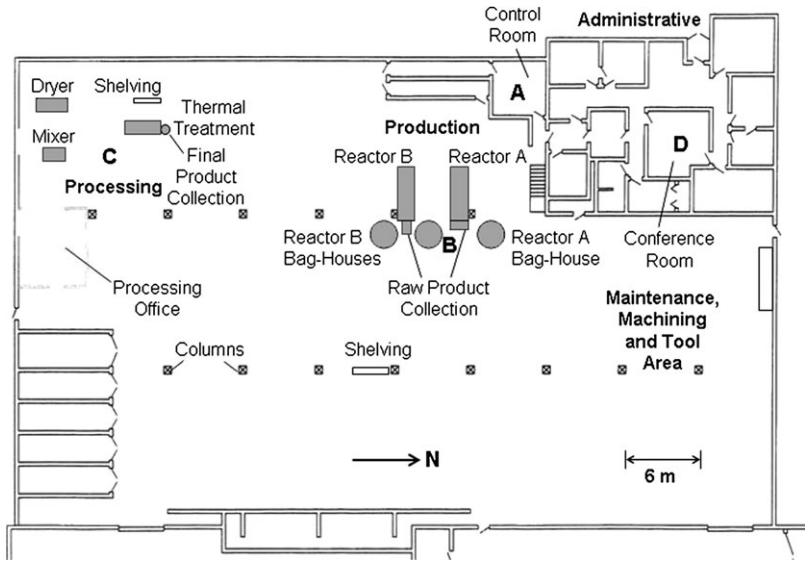

Fig. 1. A floor plan of the facility indicating approximate positions of processes and mobile sampling locations (A through D). Sampling probes were generally oriented toward and within a few feet of processes under investigation.

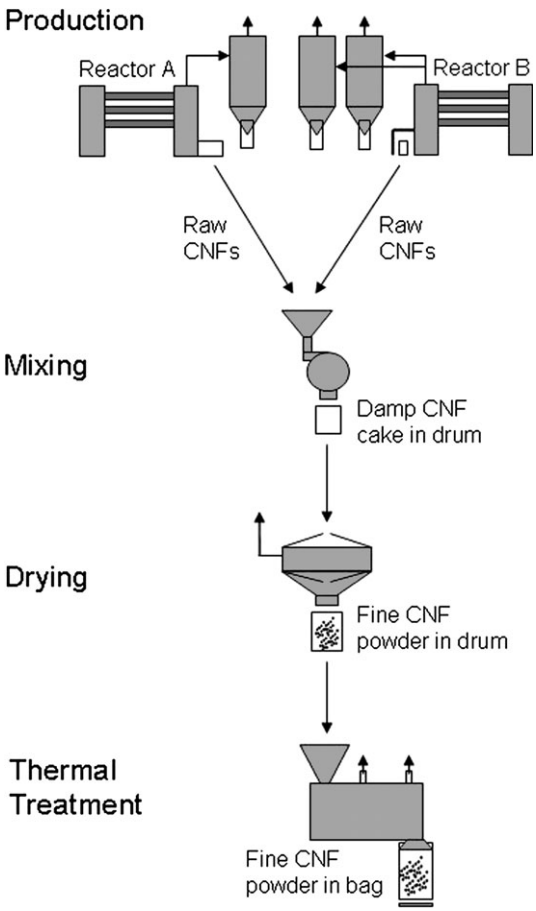

Fig. 2. Process flow diagram. In each instance, materials were manually conveyed and loaded for subsequent operations. Once thermal treatment was completed, bagged CNF product was manually unloaded, weighed, tamped, and the collection bag closed.

truck was present but was not considered a significant particle source, whereas similar combustion-based vehicles (propane, gasoline, or diesel powered) may generate significant quantities of ultrafine particles (Kuhlbusch *et al.*, 2004; Evans *et al.*, 2008). In an earlier study (Heitbrink *et al.*, 2007), battery-powered vehicles were in use without notable elevations in particle number concentrations.

METHODS

Portable instrumentation

Measurements of particle number concentration were performed with a CPC (CPC 3007; TSI Inc., Shoreview, MN, USA), with the working fluid regularly replenished. Response of the 3007 is linear to particle concentrations below $\sim 10^5$ particles cm^3; however, counting coincidence errors are introduced above this value (Hämeri *et al.*, 2002). Therefore, in environments where high particle number concentrations may be encountered, dilution is often required, and initial measurements made as part of an earlier walk-through survey of the facility obviated this need. Simple portable solutions are preferred in these applications; therefore, the dilutor consisted of a high efficiency particulate absorption (HEPA) filter cartridge (Whatman 6702-3600), with a single orifice (drill size #70, 0.028″ or 0.7112 mm diameter) drilled through the end cap. Similar devices have been used to perform high concentration measurements with the 3007 in automotive production environments (Peters *et al.*, 2006; Heitbrink *et al.*, 2007; Evans *et al.*, 2008).

A dilution ratio of ~90:1 was achieved and determined experimentally pre- and postsampling in a manner described by Peters *et al.* (2006). Briefly, this was calculated by successive addition and removal of the dilutor from the CPC inlet in a stable submicrometer particle concentration environment (i.e. distant from local particle sources such that large deviations in total particle counts over several minutes were not observed). The conference room (Fig. 1, Location D) was selected for this purpose. A consistent dilution ratio was obtained pre- and postsampling; however, it should be noted that the dilution ratio may be subject to variation if the filter media becomes heavily laden with particulate. Similar devices utilizing capillaries rather than orifices have also been reported. Although orifice size may be carefully controlled, with an extended length and residence time within the capillary, diffusional particle loss to the inner surfaces may contribute to a nonlinear relationship with concentration (Knibbs *et al.*, 2007).

Real-time respirable mass estimates were obtained using a photometer (DustTrak Model 8520; TSI Inc.), with the 10-mm Dorr-Oliver cyclone providing a respirable size-selective inlet at 1.7 l min^{-1} sampling flow.

Active surface area measurements were provided by a diffusion charging (DC)-based instrument (DC 2000 CE; EcoChem Analytics, Murrieta, CA, USA). The DC response has been compared with that of other methods (Ku and Maynard, 2005). The DC has provided active surface area measurements within automotive engine manufacturing facilities (Heitbrink *et al.*, 2009) and for monitoring diesel engine exhaust exposure (Ramachandran *et al.*, 2005).

A photoelectric aerosol sensor or PAS (PAS 2000 CE; EcoChem Analytics) was used to provide the photoelectric response of particles within the facility in real time. An overview of the PAS is provided by

Burtscher (1992) and Siegmann *et al.* (1999). Briefly, the PAS responds to aerosols from incomplete combustion, for example, and, with a low work function, is particularly sensitive to particle-adsorbed polycyclic aromatic hydrocarbons or PAHs. At a higher work function, the signal is mostly determined by elemental carbon. The presence of PAHs on preliminary air samples, taken as part of an earlier walk-through survey, suggested that the PAS may be a useful tool in this facility. In a similar application to our own, the PAS was used to indicate the presence of soot (containing fullerenes) during the harvesting of product from electrical arc reactors in a small nanomaterial facility (Yeganeh *et al.*, 2008). Both the DC and the PAS operated at 1.0 l min^{-1}. The operating principles of both instruments and their combined use are discussed by Ott and Siegmann (2006).

Air quality measurements were conducted with a Q-Trak Plus (Model 8554; TSI Inc.) and included relative humidity, temperature, carbon monoxide (CO), and carbon dioxide (CO_2). CO and CO_2 measurements may often be used to indicate the presence of combustion products in the workplace, but by association may also indicate the presence of combustion-derived ultrafines. For example, alloy pouring and exhaust from a propane-fueled vehicle resulted in elevations in both particle number and CO concentrations within a foundry (Evans *et al.*, 2008).

Particle sizing instrumentation

Particle size distributions from 7 nm to 10 μm aerodynamic diameter were obtained with an ELPI (Dekati Ltd, Tampere, Finland) operating at a nominal 10 l min^{-1}. The ELPI is a real-time cascade impactor utilizing DC and electrometer detection. An operational overview is discussed in Baltensperger *et al.* (2001). An effective aerosol density of 1.0 g cm^{-3} was assumed in estimating aerosol charging efficiencies in addition to correcting for both diffusional and space charge losses. In a similar manner, the ELPI was previously used in automotive manufacturing environments to characterize the particle size profiles of identified contaminant sources (Heitbrink *et al.*, 2007; Evans *et al.*, 2008). Oiled sintered metal impaction substrates were utilized to minimize particle bounce and reentrainment. In this instance, the external vacuum pump supplied with the ELPI (Leybold-Sogevac SV25-10991) was replaced with a dry scroll pump (SH-110, Varian Inc. Lexington MA) to reduce weight, noise, and power requirements.

Mobility equivalent particle size distributions between 5 and 500 nm were obtained with an FPSS (DMS50; Cambustion Ltd, Cambridge, UK) operating at a nominal 6.5 l min^{-1}. The DMS50 FPSS has a built-in dilution device, which may be user actuated during use but was not required during this study.

Data logging

On board data logging capabilities were utilized for the CPC, DustTrak, DC, PAS, and Q-Trak Plus, and the shortest log time intervals were selected: 1 s for the CPC and DustTrak, 10 s for the DC and PAS, and 1 s for the Q-Trak Plus. A single laptop computer with software (ELPI VI 4.0 and DMS500 UI v2-08) was used for control and data acquisition from both the ELPI and the FPSS, respectively. Raw size distribution data were collected every 1 and 2 s from the ELPI and FPSS, respectively. All instruments were time synchronized with the laptop prior to the commencement of sampling.

Workplace sampling platform

A custom mobile particle measurement platform (Fig. 3) was used to house and power particle monitoring equipment and ancillaries at given locations. Being vertically arranged, the platform provided a smaller footprint, greater maneuverability, and carrying capacity over previous commercially available carts (e.g. Peters *et al.*, 2006). Mobile power was provided through deep-cycle marine batteries and an inverter, providing several hours of uninterrupted instrument operation. With a reduced platform footprint, batteries and pump were located at the base to ensure a sufficiently low center of gravity.

Particle sampling inlets

Spatial variation in particle concentration over short distances, and, in particular, close to sources, can be considerable in workplace environments (Brouwer *et al.*, 2004; Peters *et al.*, 2006; Heitbrink *et al.*, 2007; Evans *et al.*, 2008). In such situations, instruments placed in general proximity to each other may experience substantial discrepancies in sampled concentrations. For example, large concentration differences were encountered by investigators making comparative measurements in carbon black manufacturing facilities (Kuhlbusch *et al.*, 2004), and close attention to these differences is required if quantitative comparisons between instruments and particle metrics are to be reliably conducted in the workplace.

To ensure that the same aerosol was presented to the instruments, a sampling manifold was installed to the underside of the top surface of the platform. This single line supplied sampled air to instruments

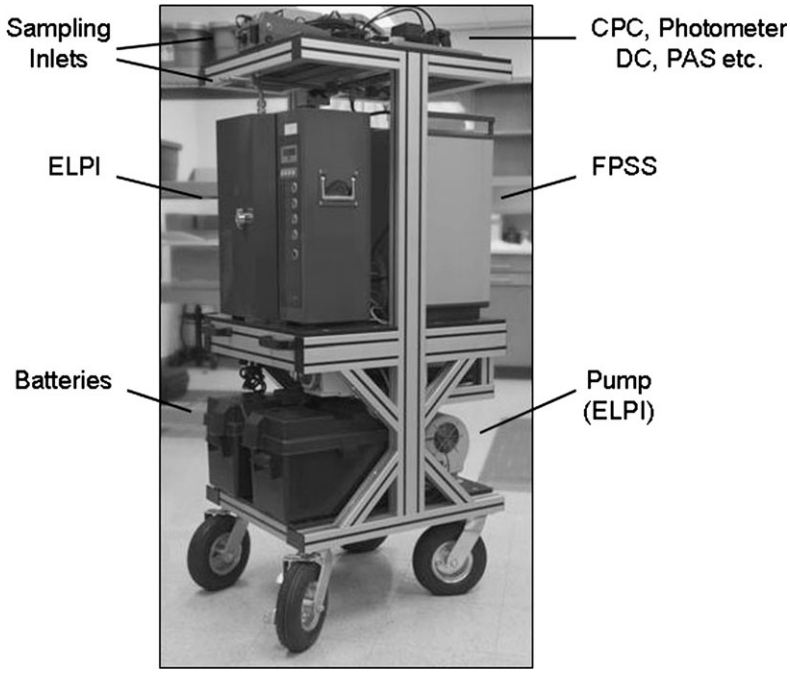

Fig. 3. The mobile aerosol sampling platform used by the authors for detailed workplace investigations as described.

responding primarily to submicrometer particle sizes, including the FPSS, CPC (with dilutor), DC, and PAS. The manifold consisted of a thin-walled stainless steel tube with a sharp beveled entry. In addition, stainless steel tube fittings and a flow splitter (3708; TSI Inc.) were utilized, with each instrument connected through short lengths of flexible conductive silicone tube.

Since inertial particle loss required consideration when sampling with the ELPI (particles up to 10 μm aerodynamic diameter), it was equipped with its own thin-walled inlet with sharp beveled entry and gentle 90° radius. The entry was positioned parallel to and within 50 mm from the manifold. In the worst case, at a diameter of 10 μm, particle losses were calculated at $<7\%$ (Brockmann, 2001). The DustTrak utilized a size-selective inlet (Dorr-Oliver cyclone) positioned within 150 mm of both manifold and ELPI inlets. Considered as area or static sampling, at $\sim$1.5 m from ground level, inlets were at a height representative of an observer's 'personal breathing zone' (Leidel *et al.*, 1977; Vincent, 1995, 2007).

Facility locations

Sampling locations are annotated in Fig. 1. Simultaneous measurements on 14 December 2007 were first conducted in the production control room (A) from $\sim$11:25 to 12:20, then adjacent to Reactor A in the fiber production area (B) from $\sim$12:20 to 13:10, subsequently in the processing area (C) from $\sim$13:10 to 16:40, and finally in the conference room (D) from $\sim$16:40 until sampling concluded. Movement from one location to the next took <1 min.

RESULTS AND DISCUSSION

CNF photometer calibration

Since particle size distribution and composition of airborne material may influence photometer response (Gebhart, 2001), measurements conducted with the photometer are considered useful for monitoring the 'relative changes' in mass concentration in a workplace rather than considered 'absolute' values. By default, the photometer comes complete with a factory calibration using the respirable fraction of standard ISO 12103-1, A1 test dust, formerly Arizona Road Dust (TSI, 2006). By several successive redispersions of milligram quantities of powdered CNFs within a small laboratory chamber, photometer response was compared against respirable mass concentration (GK2.69 cyclone; BGI Inc., Waltham, MA, USA), with CNF mass determined by gravimetric analysis [NIOSH 0600; National Institute for Occupational Safety and Health (NIOSH), 1998].

Photometer response was found to be proportional to the gravimetric mass concentration for respirable CNFs in the range 0–8 mg m^{-3}. However, some variation was noted and likely due to a combination of the efficacy of powder dispersion (i.e. some variation in particle size distribution between individual tests), the relative performance of the two respirable cyclones, and nonuniformity in concentration initially introduced into the chamber through dispersion. Linear regression provided a one-to-one relationship ($n = 9$, gradient of 0.99), with an R^2 value of 0.79, indicating that the factory calibration (performed shortly prior to this study) provided a reasonable estimate of respirable CNF mass concentration. No further calibration or correction factor was required for data collected in the facility.

Significant events

Particle and gas emissions measured at various locations (A through D) are presented as time series in Fig. 4. Notable events (I through IV) in the processing area (Location C) are marked as shaded areas and merit further examination and discussion with respect to corresponding instrument responses.

Event I: Manual bagging of final product. A transient increase in respirable mass concentration occurred at ~13:35, with a corresponding small increase observed in photoelectric response. Elevations were the result of the change-out of the collection bag (following thermal treatment) containing ~7 kg of CNFs. Emissions from this event were almost entirely due to aerosolized CNFs (dark visible airborne plume present). Tamping of the bag to settle contents (so that it could be adequately closed) and subsequent closing dispersed CNFs through the bag opening into the workplace. The photograph in Fig. 5a was taken just prior to a similar tamping task. Reduction in worker exposure through implementation of careful work practices or appropriate engineering controls would benefit this operation (see Appendix 1 for further discussion).

Event II: Opening of dryer and manual redistribution of CNF product. Shortly following Event I, two prominent transient increases in photoelectric response occurred at ~13:40 and 14:00, and modest simultaneous elevations in both active surface area and particle number concentrations were observed. These emissions were caused by the opening and manual redistribution of partially dried CNF product within the dryer by the processing operator. Note that no respirable mass elevation was observed during these operations, suggesting that significant quantities of CNFs were not emitted into the workplace. Small perturbations in CO_2 concentration were also observed. If natural gas combustion derived, a minor ultrafine particle contribution may also be expected.

Photoelectric response is highly influenced by particles possessing surface-laden PAH components (Baltenspeger *et al.*, 2001). A weak transient photoelectric response was observed in Event I during bagging. In contrast, strong responses were observed for the dryer emissions. These latter particles were likely derived from fiber-borne PAHs initially formed during fiber synthesis (Birch *et al.*, in preparation) and subsequently volatilized through the drying cycle. These particles were not CNFs but likely condensation products consisting of organic compounds with a PAH component. Emission controls (total enclosure with exhaust ventilation) appeared to be performing adequately when the dryer was closed, but notable transient increases in photoelectric response seen for short periods after opening of the dryer apparatus suggests release of PAH-containing particles.

During the period between Events II and III (Fig. 4), both drying and thermal treatment were in full progress. The last batch of CNFs passed through the thermal treatment at ~14:45, the equipment was allowed to cool, and ultrafine particle number concentrations in the processing area were subsequently observed to decline from a general maximum from that point forward.

Event III: Dumping of dried product. A sudden temporary elevation in particle number concentration appeared to occur simultaneously with the largest elevation in respirable mass concentration (at ~15:40) in Fig. 4. However, although a strong elevation in respirable particle mass appeared to occur during the same short period as corresponding increases in photoelectric response, active surface area, and particle number, one should not necessarily infer that observed responses are due to the same particles. Triggered by opening the dryer and subsequent dumping of 15 lb (7 kg) of dried product into an open lined drum below, the respirable mass elevation was almost entirely due to CNF particle release. However, elevations in active surface area, photoelectric response, and particle number were likely due to emissions of particles containing condensable PAH volatilized through the heated drying process (more modest elevations in particle number were observed on two earlier occasions described in Event II). During Event II, two successive sharp increases in photoelectric response were observed, but a concomitant increase in particle mass was not. Small perturbations in CO_2 concentration (Fig. 4) were also observed at ~15:40, with natural gas combustion being the most likely cause.

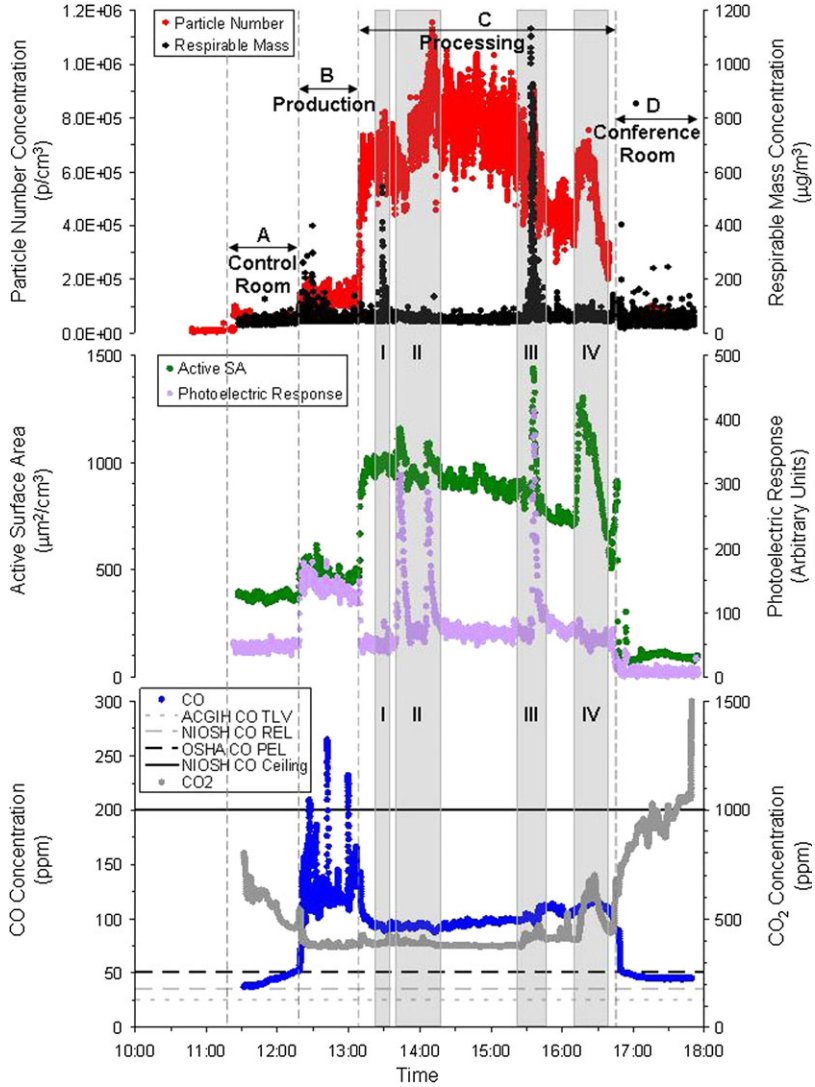

Fig. 4. Time series of particle number and respirable mass (upper), active surface area and photoelectric potential (center), and CO and CO_2 concentrations (lower) at four locations: A, control room; B, production; C, processing; and D, conference room. See floor plan (Fig. 1) for sampling locations. Shaded areas denote specific events in the 'processing' area C that resulted in marked increases in one or more monitored metrics. Events were bagging final product (I), opening of dryer (II), dumping dried product (III), and operating gas heater (IV).

Dumping of product from the dryer into a lined drum below resulted in the largest transient elevation in respirable mass concentration (1.1 mg m^{-3}), potentially exposing workers to CNFs. The base of the dryer and an adjacent empty drum are shown in Fig. 5b. Environmental release of CNFs can be minimized through the use of engineering controls (see Appendix 1 for further discussion).

In addition to the initial airborne release of material, cleanup of spilled material from the dumping operation also contributed small elevations in respirable mass concentration. Improved work practices and the development of procedures to clean up spills using a HEPA vacuum or wet methods could help reduce exposures. A small elevation observed at 15:55 in Fig. 4 was due to the sweeping of previously spilled material under the dryer by a dry floor squeegee. Subsequent HEPA vacuum use (15:58–16:01) appeared not to elevate respirable mass concentrations, suggesting relatively efficient capture.

Event IV: Operation of a radiant gas heater. At ~16:12 (Fig. 4), an interior roof-mounted gas-fired

a

b

radiant heater was ignited by the processing operator to provide supplemental heat in the processing area locale and was subsequently extinguished at ~16:30. A rapid increase in CO_2 concentration derived from this combustion process was observed. Note that corresponding increases in particle number concentration and active surface area were also observed. A rapid decline in particle number, active surface area, and CO_2 concentrations was subsequently observed following the extinguishing of the heater at 16:30. However, during this event, no notable increase was observed for respirable particle mass or photoelectric response, suggesting that in combination, these metrics may be useful in differentiating a relatively clean combustion particle plume, such as those from natural gas from other particle sources.

Locations and contaminant sources

With the notable exception for CO_2, the conference room was the cleanest of indoor locations monitored for contaminants. Rapid elevation and greatest concentrations of CO_2 were due to a number of individuals cleaning/packing equipment at the end of the day. The control room, where sampling commenced, was generally elevated in contaminant concentrations relative to the conference room but less contaminated than locations in the manufacturing area. Of the production and processing areas, particle number, transient respirable mass concentration elevations, and active surface area appeared greatest in the processing area. In contrast, general (nontransient) photoelectric response and CO concentrations were generally greatest in the fiber production area.

Both the dryer and the furnace/stripper (thermal treatment) were in close proximity, without physical barriers between them and operations ran concurrently over a period of several hours. However, the dominant source of ultrafine particles appeared to emanate from the furnace/stripper during high-temperature thermal treatment. Because ultrafine particles emitted from the dryer likely contained PAHs (Fig. 4, Events II and III), the absence of general elevation in photoelectric response in the processing area (similar to photoelectric response in the control room) suggests that for the most part, general elevations in ultrafines were not likely from the dryer.

Only on the noted occasions that the dryer was opened, did simultaneous and transient elevations in photoelectric response and active surface area concentrations result in addition to modest increases in particle number. Furthermore, the last batch of CNFs passed through the thermal treatment at ~14:45, and the ultrafine particle concentrations in the processing area were subsequently observed to decline from a general maximum observed during that period. General elevation in photoelectric response was additionally observed in the fiber production area, close to the reactors. Elevation in photoelectric response was likely due to particles with a PAH component in this locale, emitted directly from fiber synthesis operations.

It should be further noted that observed elevations in ultrafine particle concentration in the processing area were not from CNFs but rather from by-products formed through high-temperature thermal processing of the CNFs (Birch *et al.*, in preparation). Because measures were in effect to exclude oxygen and maintain an inert atmosphere during high-temperature thermal treatment, ultrafine particles were not combustion derived. Relatively consistent baseline CO_2 concentrations observed in both the fiber production and the processing areas further supports this argument.

From the perspective of direct monitoring of airborne CNF release into the workplace, respirable particle mass estimated by the photometer appeared to be the most useful and practical metric. Elevations or peaks in respirable mass concentration closely coincided with the transfer or handling of material in the open workplace. The strongest of those elevations were associated with the dumping of product after drying (Fig. 4, Event III) and the manual change-out and closing of bags of final treated CNF product (Fig. 4, Event I, and see photograph in Fig. 5a). Note that dark visible airborne clouds of CNFs were also observed on these occasions indicating the presence of large agglomerated particles. Although data presented in this article cover only a single shift, further stationary direct-reading monitoring on subsequent days indicated that CNF handling activities were directly responsible for

Fig. 5. (a) Processing operator exchanges collection bag containing ~7 kg of thermally treated CNF product in the vicinity of Position C in Fig. 1. The bag was purged with an inert atmosphere during filling. Tamping product and subsequent closing of bag resulted in significant CNF release (Event I in Fig. 4). (b) An empty collection drum adjacent to the dryer base. Once the drying cycle was complete, dumping of dried CNFs from the dryer above into the bag-lined collection drum below resulted in the largest transient increase in respirable mass concentration observed (Event III in Fig. 4). A canvas flange can be observed at the base of the dryer to assist in reducing the gap between dryer base and drum. This may not have been performing adequately for this operation.

transient mass concentration increases in the workplace. In addition, through full/partial shift integrated personal and area monitoring, sufficient respirable CNF mass was collected for quantitative and selective personal exposure determinations (Birch *et al.*, in preparation). Direct-reading measurements conducted and reported in this article provide insights into how these exposures occurred, yet worker exposures are best quantified through more selective approaches in the breathing zone. Furthermore, microscopy analysis through size-selective area sampling (Birch *et al.*, in preparation) indicated that large fiber bundles were present, further supporting findings here that particle mass may be a more practical metric for monitoring CNF emissions and exposure in this facility.

Particle number concentration and active surface area concentrations were generally greatest in the processing area. In general, active surface area concentration follows particle number more closely than particle mass (Heitbrink *et al.*, 2009) because the diffusion charger responds most strongly to sub-100-nm particles (Ku and Maynard, 2005).

In summary, integrated particle number and active surface area concentrations (determined by a CPC and DC in this study) were not particularly useful in assessing the contribution of emissions from CNFs in this workplace since these measurements were dominated by ultrafine particle emissions rather than by CNFs. A less expensive and simpler instrument such as a photometer, providing estimates of particle mass, may be more appropriate in this application. Particle number concentrations spanned from 9.0×10^4 to 1.15×10^6 cm^{-3} in the manufacturing areas. In a similar manner, active surface area concentrations due mainly to ultrafine particle emissions ranged from 430 to 1440 μm^2 cm^{-3}. When assessing emissions and potential worker exposure, multiple constituents of the mixed exposure should perhaps be considered, and these metrics may warrant further merit in this instance.

Potential pitfalls in workplace application of direct-reading particle counting

A current emphasis appears to be placed on direct-reading particle counting within the industrial hygiene community for screening nanotechnology workplaces and emission/exposure assessment (e.g. Methner *et al.*, 2010) and/or assessing the effectiveness of engineering controls (e.g. Old and Methner, 2008). This approach, although straightforward, may be a rather too simplistic for universal application. Potential errors are introduced when transient changes in particle background, simultaneous emission of ultrafine particles, or the influence from other particle sources are present. These confounding factors may not be recognized at the time, and in such instances, it may be difficult to properly proportion the nanomaterial contribution from a particular process or task. The suggested approach of deriving a mean average background concentration from several spot measurements and subtracting from the 'process' (e.g. Methner *et al.*, 2010) does not adequately address any of these issues.

Further potential errors relate to an expectation that all particles observed as a transient concentration elevation in response to a particular event or task are due to engineered nanomaterials. An example from the present study is the dryer dump event earlier discussed. A large transient particle number concentration increase was observed with this event as CNFs were dumped from the dryer to a collection vessel. The transient increase in particle number was not due to CNFs, but rather, condensable ultrafine particles emitted as the dryer apparatus was opened and fugitive emission controls were temporally breached. Using only particle counting as a guide, this critical distinction between particle sources would not have been determined using current approaches (e.g. Methner *et al.*, 2010). Opening of the dryer for manual redistribution of partially dried CNFs also generated ultrafine particle emissions, yet little if any CNFs. A good understanding of workplace emissions is an essential prerequisite to reducing exposure because recommended approaches to mitigate these related but very different particle emissions may vary considerably (see Appendix 1 for discussion of exposure controls). Careful interpretation is required when relying on simple measurements in the assessment of complex systems.

CO emissions

Results for CO monitoring are also presented as a time series in Fig. 4. Elevated CO concentrations in this facility were found to be of particular concern but were not the primary focus of this study; therefore, further discussion is provided in the Appendix 1. The peak concentration observed was 265 ppm in the production area, with mean average concentrations of 44, 130, 99, and 47 ppm observed in the control room, production area, processing area, and conference room, respectively, over the periods sampled in these locations. Thermal decomposition of the carbonyl catalyst precursor during fiber synthesis was the likely source.

Particle size distributions for ultrafine particle sources

Measurements conducted with the ELPI (aerodynamic diameter) and FPSS (mobility equivalent diameter) provided number-weighted particle size distributions over the entire sampling period, giving a combined size range spanning 5 nm to 10 μm. By careful observation and interpretation of data presented in Fig. 4, as earlier described, particle sources and plumes were identified. Size distributions were obtained as mean average measurements over periods present in these locations and are presented in Fig. 6. In the case of thermal treatment (at the furnace/stripper), averaging was taken over those periods not influenced by Events I through IV since elevations observed during these periods were from other sources.

In contrast, since relatively transient, event timing was used to identify pertinent plume data in the dryer plume and gas burner plume cases, and the results are presented over shorter duration (several minutes) in Fig. 6. Concentration range bars were not included for clarity, but concentrations varied considerably in the case of the processing area, as evidenced by the variability in the CPC-derived particle number concentrations presented in Fig. 4, but relatively stable, for instance, for the outdoor background measurements.

Dominant sub-10-nm modes were noted for the thermal treatment and production emissions, suggesting freshly nucleated particles. Dryer plumes were dominated by the thermal treatment emissions when present, so they exhibited a similar size profile. However, small concentration increases between 50 and 200 nm are just perceivable, consistent with condensation particle emissions from the dryer. Gas burner emissions exhibited an additional mode between 15 and 25 nm and concentration elevations in the 20–80 nm size range above those seen previously for thermal treatment or dryer emissions. Similarly sized modes were previously observed (Heitbrink *et al.*, 2007). A distribution from outdoor background (semirural location and upwind of the facility) provided the lowest concentrations observed in the study. FPSS data above ∼100 nm (Fig. 6) were not plotted because data were influenced by an erroneous electrometer offset; however, the ELPI provided sufficient data to adequately cover this size range.

Particle size distributions for CNFs

Since other particle sources in the facility dominated on a particle number basis, extracting specific size information for CNFs (by number) was challenging. However, careful time alignment with observations assisted in identifying events when CNF plumes were known to be present and respirable mass estimates, provided by the photometer, were particularly useful in identifying these periods. By careful selection of appropriate baseline

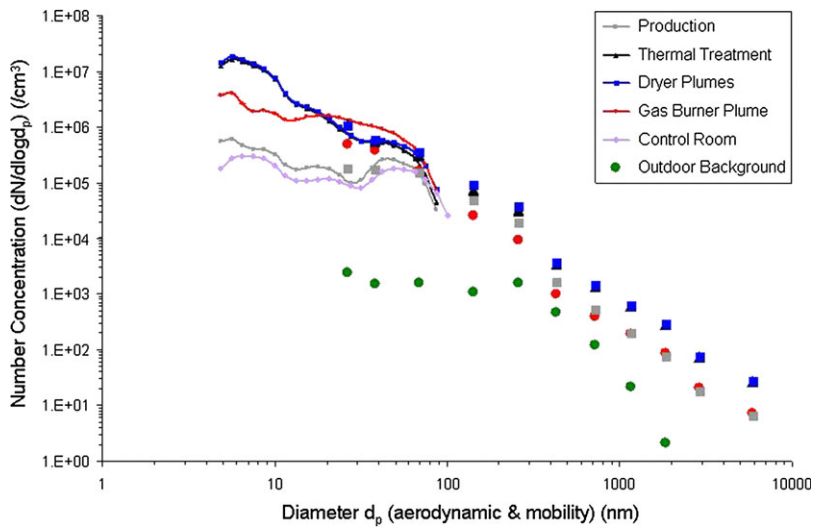

Fig. 6. Particle size distribution comparison (weighted by number) for ultrafine particle sources at the facility. Measurements were conducted by aerodynamic diameter (ELPI) and mobility equivalent diameter (FPSS). Data from the FPSS were plotted as lines (see legend). For the ELPI, corresponding impactor stages were used and data (geometric mean diameters) plotted as individual points of the same color. A measurement artifact (electrometer offset) influenced FPSS measurements above ∼100 nm, so data were not included.

distributions, net changes in particle size distributions from both the FPSS and the ELPI were derived and are presented in Fig. 7. Subtraction of the CNF plumes from baselines negated the effect of the erroneous electrometer offset for the FPSS data >100 nm since this was consistent throughout. Baseline distributions were derived as a mean average during a relatively stable period (typically a few minutes) just prior to known CNF emissions. Raw CNF distributions were averaged over a period of several minutes when the plume was known to be present.

A larger quantity of CNFs was released on a respirable mass basis (see Fig. 4) for the dryer dump event over the bag change event. Respectively, a greater elevation in particle number concentrations by size was correspondingly observed in the size distribution data. During both events, CNF plumes exhibited dominant modes weighted by number between 200 and 250 nm as both mobility equivalent (FPSS) and aerodynamic diameters (ELPI). ELPI measurements exhibited shoulders in the overall distribution at this size but corresponded closely to measurements from the FPSS, with the latter providing greater sizing resolution. The close agreement between these two different, but complementary, sizing techniques provides a greater level of confidence in the presented CNF size data. A secondary mode (observed as shoulders) between ~1 and 3 μm aerodynamic diameter was also observed in the ELPI size distributions weighted by number for both CNF plumes. The photometer (response proportional to mass) likely responded most strongly to particles in this size range.

Because both aerodynamic and mobility equivalent diameters appear very similar for the 200- to 250-nm CNF mode, effective particle densities at or close to unity are implied. For a theoretical discussion on the interrelationships between mobility equivalent, aerodynamic diameters, and effective densities, see DeCarlo *et al.* (2004). In a prior study (Ku *et al.*, 2006), CNF particles generated through laboratory agitation of bulk powder provided effective densities between 0.85 and 0.75 g cm^{-3} at 200 and 250 nm, respectively. Our findings are generally consistent with these earlier observations. A decrease in the effective density of particles with larger diameters is anticipated (greater divergence in mobility and aerodynamic diameters), as more complex and open structures are observed (Ku *et al.*, 2006). CNF particle structures in the 200–250 nm size range consisted mostly of clusters of fibers with some single fibers also observed (Ku *et al.*, 2006). Similar structures were observed from CNF plumes in this workplace (see Birch *et al.*, in preparation).

Estimation of CNF particle number concentrations

Since integrated particle number concentration measurements provided by the CPC were dominated by other sources (Fig. 4), it is impossible to obtain the contribution from CNFs solely through these

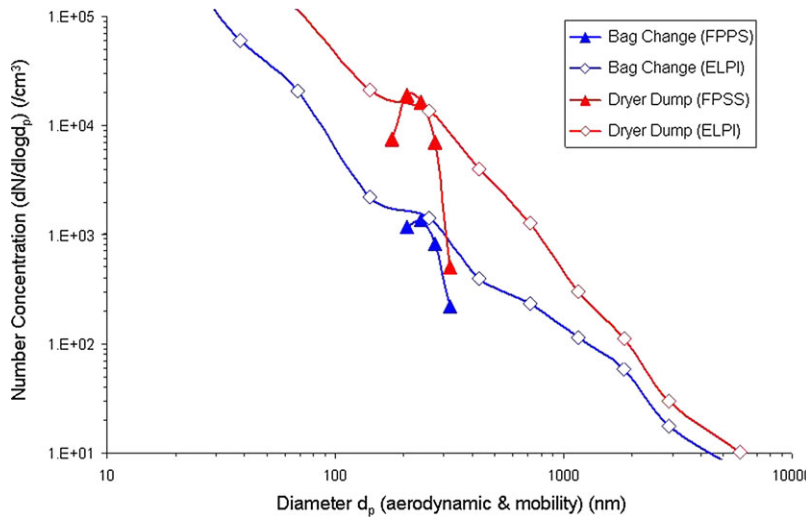

Fig. 7. Particle size distributions (weighted by number) for significant CNF plumes observed in the facility (bag change and dryer dump) in the vicinity of Location C in Fig. 1. Measurements were by aerodynamic diameter (ELPI) and mobility equivalent diameter (FPSS). Distributions were derived by selecting and subtracting appropriate baselines from plumes and are therefore derived from net changes in particle concentration.

measurements. However, by utilizing size distribution data, one may estimate particle number concentration increases for the two notable events that precipitated major releases of airborne CNFs. FPSS particle size distributions for CNF plumes were utilized (Fig. 7) since these data possess finer size resolution than corresponding ELPI data. The bag change event resulted in an estimated 230 cm^{-3} transient elevation in particle number concentration from CNFs and the dryer dump event an estimated 3130 cm^{-3} elevation. These values need to be compared to a mean average particle number concentration of 6.53×10^5 cm^{-3} (obtained with the CPC) observed in the processing area over the period measurements that were conducted in this location. On a particle number basis, CNF plumes made up ~0.035 and 0.48%, respectively, of mean average particle number concentrations, illustrating the challenges and potential inaccuracies in making such measurements. For example, had the transient particle number concentration increase of between 3.0 and 3.5×10^5 cm^{-3} above baseline associated with the dryer dump event been erroneously and solely attributed to CNFs, a potential two orders of magnitude error in estimated CNF number concentration would have resulted.

CONCLUSIONS

A mobile particle sampling platform furnished with direct-reading instrumentation was employed in the characterization of particulate emissions within a CNF manufacturing facility. Through comparison of simultaneous metrics (particle number, respirable mass, active surface area, photoelectric response, CO, and CO_2), CNF, combustion, noncombustion, and PAH-containing particle plumes were differentiated from one another. Ultrafine particle sources included thermal treatment of CNFs, CNF drying, CNF synthesis, and a radiant gas-fired heater. Elevated particle number concentrations, up to 1.15×10^6 cm^{-3}, were found within the facility but were not due to CNFs. Ultrafine particle emissions, released during thermal treatment of CNFs, were primarily responsible for the high particle number concentrations observed. Respirable particle mass appeared to be the most useful metric of those applied for the direct-reading monitoring of CNF emissions in this facility. The transfer or dumping of dried CNFs from a dryer to a collection vessel, and subsequent bag change-out of final product, contributed the largest transient increases in respirable mass concentrations, with concentrations during these events exceeding 1.1 and 0.5 mg m^{-3}, respectively. The photometer, with default factory calibration, provided a reasonable estimate of respirable CNF concentrations and will likely be the instrument of choice for direct-reading monitoring of CNFs in future studies of this type.

Particle size distribution measurements (weighted by number) indicated that CNFs exhibited a primary mode between 200 and 250 nm. Both aerodynamic and mobility equivalent diameters were similar, indicating particle effective densities at or close to unity. Particles derived from thermal treatment, drying, and fiber synthesis possessed a significant primary sub-10-nm mode indicating freshly nucleated particles. The radiant gas heater, in contrast, possessed a notable mode between 15 and 25 nm.

Significant emissions of CO into the workplace were also evident. Transient concentrations of up to 270 ppm were observed in the fiber synthesis location with thermal decomposition of the metallocarbonyl catalyst precursor likely the underlying cause.

Direct-reading monitoring by multiple instruments contributed significantly to the understanding of emissions and the potential for worker exposure within this facility. Future implementation of effective exposure controls (examples of which are described in the Appendix 1) will likely result in their reduction.

FUNDING

NIOSH Nanotechnology Research Center under intramural research projects 927Z2MK and 927Z8VM.

Acknowledgements—The authors are thankful for the valuable conceptual/technical contributions and assistance provided by the late Paul A. Baron, Cynthia Roettgers, Leonid A. Turkevich, Pramod S. Kulkarni, Toni Ruda-Eberenz, Jerry L. Kratzer, Daniel R. Farwick, Ronald J. Kovein, and Magdalena A. Steciuk. The authors wish to acknowledge the support and willing cooperation from the management and staff of the facility described.

Disclaimers—The findings and conclusions in this report are those of the authors and do not necessarily represent the views of the NIOSH. Mention of product or company name does not constitute endorsement by the Centers for Disease Control and Prevention.

APPENDIX 1

Process descriptions

Fiber production. Vapor-grown CNFs were continuously produced in two electrically heated reactors, A and B, at temperatures exceeding 1000°C. Pyrolysis of natural gas took place in the presence of a metallocarbonyl catalyst precursor within a reducing atmosphere. Once formed, crude CNFs were settled and harvested through extruders. At Reactor A, compressed product was manually broken away

and lifted out of an open collection trough at ~30-min intervals and placed into open plastic lined boxes for further processing. Reactor B was of a later design. Product from Reactor B was automatically fed into a similarly lined open box, falling ~2 ft. Both harvesting procedures were conducted in the open workplace and the reactors operated under positive pressure. Effluent gases were subsequently passed through reverse pulsed fabric filter baghouses to remove remaining product prior to external discharge through exhaust ventilation. Separate baghouses were utilized for each reactor.

On regular occasions, product bags were manually closed, tied, and carried to the processing area. On a more infrequent basis, baghouse collection bags were manually replaced. General cleanup of spills and deposits on floors in the vicinity of the reactors was conducted with a HEPA filter-equipped vacuum.

Postproduction processing

Some or all of the following batch processing occurred, with some operations overlapping others in duration. Postproduction sampling took place in the locale of C in Fig. 1. Postproduction processing was at the pilot scale within this facility and intended for 'proof of concept' at moderate production rates. While processes continue to be established and refined, manual transfer of materials is necessary but, where feasible, will be designed out in favor of automated material transfer systems that expedite processing and reduce the potential for worker exposure.

Mixing. Crude CNFs were manually emptied from bags into a large hopper above a mixing unit by the processing operator. CNFs were then auger fed through the hopper base and mechanically mixed for several minutes with an aqueous solution. Upon completion of the cycle, damp CNF cake was gravity fed into a metallic drum with wheels placed below the mixer.

Drying. The operator manually scooped damp CNF cake from the drum and spread CNFs into a heated dryer (natural gas fueled). The dryer was completely enclosed and emissions were exhausted to outdoors. However, fugitive emissions were released when the enclosure was compromised through loading, redistributing, and unloading of product. The full drying cycle lasted ~4 h, at which point CNFs were dumped through hinged openings at the base of the dryer into an open bag-lined drum.

Thermal treatment. CNFs were manually loaded from bags into a second large hopper for thermal treatment. Product was then mechanically fed into the furnace and heated to several hundred degrees Celsius to remove organic compounds remaining from the previous heated drying process. Flexible ducting (100 mm diameter) was utilized to capture and exhaust visible yellow-brown emissions from ports in the apparatus. Final CNF product was collected into a plastic bag, clamped to the exit of the thermal treatment system. The thermal treatment apparatus ran continuously and remained at high temperature for several hours, but processing for a single batch of CNFs was of considerably shorter duration. The bag, resting upon a weighing scale, was manually removed, tamped, closed, and tied when filled to ~7 kg. This mass of loose powdered material filled an ~150 l volume.

Recommendations for controlling emissions and exposures

Bag change-out following thermal treatment. Exposures resulting from the manual handling of powdered materials are common in industry. Reduction in worker exposure through implementation of careful work practices or appropriate engineering controls would likely benefit the bag change-out operation following thermal treatment. Engineering solutions could include a continuous liner off-loading system (Hirst *et al.*, 2002) in which a continuous pull-down plastic bag (crimped at each end) contains any dust generated during product collection, thereby enclosing the process and reducing opportunity for worker exposure. A further exposure control option would be a ventilated bagging/weighing station (ACGIH, 2007) that draws contaminants away from the worker during manual handling activities. These engineering controls have been used in the pharmaceutical, process, and other manufacturing industries to help control exposures to workers during handling of materials. If properly designed and implemented, either of these options would likely substantially reduce the opportunity for worker exposure to airborne CNFs.

Drum filling following drying. Several examples of engineered drum or bag filling solutions have been described (Hirst *et al.*, 2002; ACGIH, 2007) and could be implemented. These engineering controls consist of enclosing the product off-loading process by temporarily sealing the drum/bag to the filling vessel above and/or overbagging through a continuous liner-type bagging system. The addition of a local exhaust ventilation hood near the drum/bag opening could capture airborne CNFs. The system exhaust flow rate may need to be carefully evaluated during pilot testing to ensure that the system maintains adequate capture while minimizing the loss of valuable product. Local exhaust

ventilation systems have been described for nanomaterial applications (e.g. Old and Methner, 2008), but important factors such as product loss, inlet optimization, the safe maintenance, or replacement of filter media were not considered in this example; however, best practice dictates these requirements for efficient and safe systems. In general, the primary design consideration for any engineered solution is that airborne process dust or displaced air (with airborne CNFs in this instance) resulting from transfer be either fully contained or safely captured.

Thermal treatment. Although ventilation controls were installed on the furnace/stripper apparatus (loose-fitting 100-mm-diameter flexible exhaust ventilation ducts located above exhaust ports), ultrafine particle emissions into the workplace occurred and varied considerably over the sampling period as evidenced in Fig. 4. The existing design of the furnace/stripper made sealing the apparatus difficult. The furnace/stripper was at high temperature, contained moving parts, and operated under positive pressure, as nitrogen was introduced to maintain an inert atmosphere. One possible option in controlling ultrafine emissions from this source would be the addition of a full or partial ventilated enclosure, such that emissions were adequately captured and exhausted from the workplace. A further option worth exploring would be the implementation of a canopy hood (ACGIH, 2007). Since emissions were hot and potentially subjected to strong thermal buoyancy effects, a control of this nature might be applicable to this operation (McKernan *et al.*, 2007). Contaminant capture velocities suitable for gas/vapor contaminants (rather than particulates) may be sufficient since particles were primarily ultrafine and thus possessed negligible inertia. Accessibility to the furnace/stripper would need to be considered as a primary factor in the enclosure or hood design.

CO emissions and potential for worker exposure

Exposure limits have been established for CO by NIOSH (1972, 1994), the ACGIH (2008), and the Occupational Safety and Health Administration (OSHA) (CFR, 1997). The current OSHA permissible exposure limit of 50 ppm is based on full shift time-weighted average (TWA) concentrations (CFR, 1997). ACGIH (2008) has established an 8-h TWA of 25 ppm. NIOSH has also published both a recommended exposure limit of 35 ppm and a ceiling limit value of 200 ppm, based on cardiovascular risk, with the ceiling not to be exceeded at any time (NIOSH, 1972). Although measurements reported in this article were based on area sampling (not personal monitoring), concentrations presented in Fig. 4 nonetheless illustrate that operators may be exposed to substantial CO concentrations. If present within the manufacturing area for a considerable portion of the working day, operators' exposures will likely exceed some or all of the occupational exposure limits noted above. For example, the NIOSH 200-ppm ceiling limit (NIOSH, 1972) was exceeded on three successive occasions during monitoring in the fiber production area (see Fig. 4). Improved sealing of the production apparatus and use of exposure controls, such as adequate localized exhaust ventilation, should also aid in reducing worker exposure to CO.

Measurements conducted in the control room, during the late morning, illustrate CO concentrations steadily increasing since commencement of production activities earlier that morning (Fig. 4). The greatest CO concentrations were in close vicinity to fiber synthesis (reactors), and the rapid changes observed are indicative of the close proximity to a strong source or sources. Thermal decomposition of carbonyl catalyst precursor during fiber synthesis with subsequent leakage of emissions through the production apparatus appeared the likely source.

In contrast, a relatively stable CO concentration was observed in the processing area. Since CO is relatively unreactive, the major loss mechanism for this contaminant is through air exchange with outdoors. As sampling ended, conference room concentrations were elevated (mean average 47 ppm) with respect to outdoor background (upwind, 0 ppm) and indicated that CO was generated entirely indoors with migration from the manufacturing to the administrative area.

REFERENCES

ACGIH. (2007) Industrial ventilation: a manual of recommended practice. 26th edn. Cincinnati, OH. ACGIH Signature Publications.

ACGIH. (2008) 2008 TLVs® and BEIs® threshold limit values for chemical substances and physical agents and biological exposure indices. Cincinnati, OH: ACGIH Signature Publications.

Baltensperger U *et al.* (2001) Dynamic mass and surface area measurements. In: Baron PA and Willeke K, editors. Aerosol measurement-principles, techniques, and applications. New York: Wiley-Interscience; pp. 387–418.

Brockmann JE. (2001) Sampling and transport of aerosols. In: Baron PA and Willeke K, editors. Aerosol measurement-principles, techniques, and applications. New York: Wiley-Interscience; pp. 143–95.

Brouwer DH, Gijsbers JHJ, Lurvink MWM. (2004) Personal exposure to ultrafine particles in the workplace: exploring sampling techniques and strategies. Ann Occup Hyg; 48: 439–53.

Burtscher H. (1992) Measurement and characteristics of combustion aerosols with special consideration of photoelectric charging and charging by flame ions. J Aerosol Sci; 23: 549–95.

CFR. (1997) 29 CFR 1910.1000, chapter XVII—Occupational Safety and Health Administration. Code of Federal Regulations, Table Z-1, limits for air contaminants. Washington, DC: US Federal Register.

Dasch J *et al*. (2005) Characterization of fine particles from machinery in automotive plants. J Occup Environ Hyg; 2: 609–25.

DeCarlo PE *et al*. (2004) Particle morphology and density characterization by combined mobility and aerodynamic diameter measurements. Part 1: theory. Aerosol Sci Technol; 38: 1185–204.

Evans DE *et al*. (2008) Ultrafine and respirable particles in an automotive grey iron foundry. Ann Occup Hyg; 52: 9–21.

Gebhart J. (2001) Optical direct-reading techniques: light intensity systems. In: Baron PA and Willeke K, editors. Aerosol measurement-principles, techniques, and applications. New York: Wiley-Interscience; pp. 419–54.

Hämeri K *et al*. (2002) The particle detection efficiency of the TSI-3007 condensation particle counter. J Aerosol Sci; 33: 1463–9.

Heitbrink WA *et al*. (2007) The characterization and mapping of very fine particles in an engine machining and assembly facility. J Occup Environ Hyg; 4: 341–51.

Heitbrink WA *et al*. (2009) Relationships among particle number, surface area, and respirable mass concentration in automotive engine manufacturing. J Occup Environ Hyg; 6: 19–31.

Hirst N, Brocklebank M, Ryder M. (2002) Containment systems: a design guide. Warwickshire, UK: Institution of Chemical Engineers (IChemE).

Holman MN *et al*. (2007) The nanotech report. 5th edn. New York: Lux Research.

ISO/TS 27687:2008. (2008) Nanotechnologies: terminology and definitions for nano-object; nanoparticle, nanofibre and nanoplate. Geneva, Switzerland: International Standard Organization.

Kisin E *et al*. (2010) Pulmonary response, oxidative stress and genotoxicity induced by carbon nanofibers. Toxicologist, 114: 169.

Knibbs LD *et al*. (2007) A simple and inexpensive dilution system for the TSI 3007 condensation particle counter. Atmos Environ; 41: 4553–7.

Ku BK, Maynard AD. (2005) Comparing aerosol surface-area measurements of monodisperse ultrafine silver agglomerates by mobility analysis, transmission electron microscopy and diffusion charging. J Aerosol Sci; 36: 1108–24.

Ku BK *et al*. (2006) In situ structure characterization of airborne carbon nanofibers by a tandem mobility-mass analysis. Nanotechnology; 17: 3613–21.

Kuhlbusch TAJ, Neumann S, Fissan H. (2004) Number size distribution, mass concentration and particle composition of PM_1, $PM_{2.5}$ and PM_{10} in bag filling areas of carbon black production. J Occup Environ Hyg; 1: 660–71.

Leidel NA, Busch KA, Lynch JR. (1977) Occupational exposure sampling strategy manual. DHEW (NIOSH) Publication No. 77-173. Cincinnati, OH: US Department of Health, Education, and Welfare, Public Health Service, Center for Disease Control, National Institute for Occupational Safety and Health.

Lux Research. (2008) Nanomaterials state of the market Q3 2008: stealth success, broad impact. Boston, MA: Available at http://www.luxresearchinc.com/.

Maynard AD, Kuempel ED. (2005) Airborne nanostructured particles and occupational health. J Nanoparticle Res; 7: 587–614.

Maynard AD *et al*. (2007) Measuring particle size-dependent physicochemical structure in airborne single walled carbon nanotube agglomerates. J Nanopart Res; 9: 85–92.

McKernan JL *et al*. (2007) Evaluation of a proposed area equation for improved exothermic control. Ann Occup Hyg; 51: 725–83.

Methner M, Hodson L, Geraci C. (2010) Nanoparticle emission assessment technique (NEAT) for the identification and measurement of potential inhalation exposure to engineered nanomaterials. Part A. J Occup Environ Hyg; 7: 127–32.

Murray AR *et al*. (2009) Oxidative stress and inflammatory response in dermal toxicity of single-walled carbon nanotubes. Toxicology; 257: 161–71.

NIOSH. (1972) Criteria for a recommended standard: occupational exposure to carbon monoxide. DHHS (NIOSH) Publication No. 73–11000. Cincinnati, OH: National Institute for Occupational Safety and Health.

NIOSH. (1994) Documentation for immediately dangerous to life and concentrations (IDLH). NTIS Publication No. PB-94-195047. Cincinnati, OH: National Institute for Occupational Safety and Health.

NIOSH. (1998) Method 0600 particles not otherwise regulated—respirable. Cassinelli ME and O'Connor PF, editors. NIOSH manual of analytical methods (NMAM). 4th edn. Cincinnati, OH: NIOSH, pp. 1–6.

Oberdörster G *et al*. (2005) Principles for characterizing the potential human health effects from exposure to nanomaterials: elements of a screening strategy. Part Fiber Toxicol; 2: 8. doi: 10.1186/1743-8977-2-8.

Old L, Methner MM. (2008) Engineering case report: effectiveness of local exhaust ventilation (LEV) in controlling engineered nanomaterial emissions during reactor cleanout operations. J Occup Environ Hyg; 5: D63–9.

Ott WR, Siegmann HC. (2006) Using multiple continuous fine particle monitors to characterize tobacco, incense, candle, cooking, wood burning and vehicular sources in indoor, outdoor, and in-transit settings. Atmos Environ; 40: 821–43.

Peters TM *et al*. (2006) The mapping of fine and ultrafine particle concentrations in an engine machining and assembly facility. Ann Occup Hyg; 50: 249–57.

Poland CA *et al*. (2008) Carbon nanotubes introduced into the abdominal cavity of mice show asbestos-like pathogenicity in a pilot study. Nat Nanotechnol; 3: 423–8.

Ramachandran G *et al*. (2005) Mass, surface area and number metrics in diesel occupational exposure assessment. J Environ Monit; 7: 728–35.

Roco MC, Bainbridge WS. (2005) Societal implications of nanoscience and nanotechnology: maximizing human benefits. J Nanopart Res; 7: 1–13.

Shvedova AA *et al*. (2005) Unusual inflammatory and fibrogenic pulmonary responses to single-walled carbon nanotubes in mice. Am J Physiol Lung Cell Mol Physiol; 289: 698–708.

Shvedova AA *et al*. (2008) Inhalation versus aspiration of single-walled carbon nanotubes in C57bl/6mice: inflammation, fibrosis, oxidative stress and mutagenesis. Am J Physiol Lung Cell Mol Physiol; 295: L552–65.

Siegmann K, Scherrer L, Siegmann HC. (1999) Physical and chemical properties of airborne nanoscale particles and how to measure impact on health. J Mol Struct; 458: 191–201.

TSI. (2006) Model 8520 DustTrak Aerosol Monitor. Operation and service manual. Shoreview, MN.

Vincent JH. (1995) Aerosol science for industrial hygienists. Oxford, UK: Pergamon, Elsevier Science Ltd.

Vincent JH. (2007) Aerosol sampling: science, standards, instrumentation and applications. Chichester, UK: John Wiley and Sons Ltd.

Wang H, Xu Z, Eres G. (2006) Order in vertically aligned carbon nanotube arrays. Appl Phys Lett; 88: 213111.

Wang H *et al*. (2007) Synthesis of aligned carbon nanotubes on double-sided metallic substrate by chemical vapor deposition. J Phys Chem C; 111: 12617–24.

Yeganeh B *et al*. (2008) Characterization of airborne particles during production of carbonaceous nanomaterials. Environ Sci Technol; 42: 4600–6.